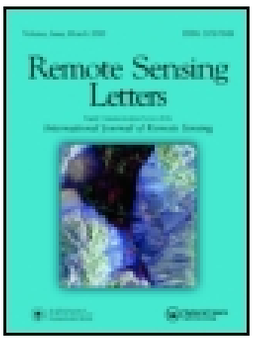

Remote Sensing Letters

ISSN: (Print) (Online) Journal homepage: https://www.tandfonline.com/loi/trsl20

Estimation of ground-level dry $PM_{2.5}$ concentrations at 3 km resolution over Beijing using Geostationary Ocean Colour Imager

Jingwei Wang & Zhengqiang Li

To cite this article: Jingwei Wang & Zhengqiang Li (2020) Estimation of ground-level dry $PM_{2.5}$ concentrations at 3 km resolution over Beijing using Geostationary Ocean Colour Imager, Remote Sensing Letters, 11:10, 913-922, DOI: 10.1080/2150704X.2020.1795298

To link to this article: https://doi.org/10.1080/2150704X.2020.1795298

Published online: 24 Jul 2020.

REMOTE SENSING LETTERS
2020, VOL. 11, NO. 10, 913–922
https://doi.org/10.1080/2150704X.2020.1795298

Taylor & Francis
Taylor & Francis Group

Estimation of ground-level dry $PM_{2.5}$ concentrations at 3 km resolution over Beijing using Geostationary Ocean Colour Imager

Jingwei Wang[a,b] and Zhengqiang Li[a]

[a]State Environmental Protection Key Laboratory of Satellite Remote Sensing, Aerospace Information Research Institute, Chinese Academy of Sciences, Beijing, China; [b]School of Surveying and Geo-Informatics, Shandong Jianzhu University, Jinan, China

ABSTRACT

In this study, aerosol optical depth (AOD) and fine-mode fraction (FMF) with a 3 km resolution are retrieved from Geostationary Ocean Colour Imager (GOCI) data using a multi-temporal method. The retrieved results are input into a physical model for estimating the fine particulate matter ($PM_{2.5}$) based on instantaneous satellite-based measurements. The other two input parameters of the model are planetary boundary layer height (PBLH) and atmospheric relative humidity (RH), which are simulated by the Weather Research and Forecasting (WRF) model and have the same spatial resolution as AOD and FMF. For better time-matching, the time of the simulated PBLH and RH is almost the same as that of the retrieved AOD and FMF, and is selected when uniform mixing of aerosols occurs within boundary layer in the afternoon. Finally, the ground-level dry $PM_{2.5}$ concentrations at a 3 km resolution are estimated over Beijing. The GOCI-estimated $PM_{2.5}$ results are validated by in situ measurements in the study area. The means of GOCI-estimated and in situ results are very close (131.2 μg m^{-3} versus 123.0 μg m^{-3}) and the correlation coefficient is about 0.84 with a linear slope of 0.81 and intercept of 31.1 μg m^{-3}, which shows good performance of GOCI in air-quality monitoring.

ARTICLE HISTORY
Received 27 March 2020
Accepted 21 June 2020

1. Introduction

The satellite-based estimation of dry fine particulate matter ($PM_{2.5}$) concentrations near the surface is urgently needed in the air-quality monitoring. To date, researchers have proposed many approaches that use the relationship between $PM_{2.5}$ and satellite-derived aerosol optical depth (AOD) to generate these estimations, in combination with employing other spatiotemporal predictors. These approaches include statistical regressions (Lv et al. 2017), chemical transport models (Pang et al. 2018), machine learning models (Park et al. 2019), physical models (Li et al. 2016), etc. The continuous renewal and improvement of the methods and techniques for $PM_{2.5}$ monitoring from space have significantly improved the capability of $PM_{2.5}$ estimation, as well as the accuracy.

CONTACT Jingwei Wang wjw_sdust@sdjzu.edu.cn State Environmental Protection Key Laboratory of Satellite Remote Sensing, Aerospace Information Research Institute, Chinese Academy of Sciences, Beijing, China

Among the existing models, physical models do not rely on the richness of historical data for sample training and can be applied to different regions to achieve the real-measurement of spatial coverage of $PM_{2.5}$. We therefore employ a physical model called $PM_{2.5}$ remote sensing (abbr. PMRS) method to estimate $PM_{2.5}$ concentrations. The PMRS method has been validated by ground-based remote sensing data and satellite-retrieved AOD data with a coarse spatial resolution of 10 km from the Moderate Resolution Imaging Spectroradiometer (MODIS). In this study, new AOD data from satellite instruments are used to further validate this method. Considering the spatiotemporal matching among input parameters in PMRS method, we apply AOD data retrieved from Geostationary Ocean Colour Imager (GOCI), which collects multispectral imagery at eight spectral channels (412, 443, 490, 555, 660, 680, 745 and 865 nm) with 500 m resolution and provides multispectral imagery of Northeast Asia region hourly from 0:16 to 7:16 Coordinated Universal Time (UTC). GOCI data over land have been applied to retrieve high temporal resolution AOD (Zhang et al. 2014). Since the AOD at less than 3 km spatial resolution may be considered as not so suitable for air-quality studies due to improper characterization of the underlying urban surfaces that resulted in significant lower signal-to-noise ratio for AOD retrieval (Munchak et al. 2013), the AOD of 3 km spatial resolution is retrieved from GOCI and used for $PM_{2.5}$ estimation with the same resolution.

The objective of this study is to provide the approach using GOCI data over land to estimate $PM_{2.5}$ concentrations and to validate the estimation. We choose Beijing area as our study area, considering that it is one of the most air polluted areas in recent years in China. In addition, Beijing has established a large-scale network to monitor ground-level $PM_{2.5}$. This allows us to use rich in situ measurements to verify the accuracy of $PM_{2.5}$ estimation effectively.

2. Methodology

2.1. PMRS method

Assume that all of particulate matters, whose hygroscopic properties are independent of aerosol size, are uniformly mixed in a homogeneous layer with layer top in planetary boundary layer height (PBLH) and that aerosol size and absorption properties are independent with height. The estimation of ground-level dry $PM_{2.5}$ concentrations can be expressed as (Li et al. 2016):

$$PM_{2.5} = AOD \frac{FMF \times VE_f(FMF)}{PBLH \times f_o(RH)} \rho_{2.5,dry} \quad (1)$$

where $PM_{2.5}$ is mass concentration (mg m^{-3}) of dry particulates near the ground; AOD is aerosol optical depth; fine-mode fraction (FMF) is AOD's fine mode fraction; $VE_f(FMF)$ is columnar volume-to-extinction ratio of fine particulates; PBLH is planetary boundary layer height (km); $f_o(RH)$ is the optical hydroscopic growth function, RH is relative humidity (from 0 to 100) of atmosphere on the ground level; $\rho_{2.5,dry}$ is density of dry $PM_{2.5}$ particulates. In the previous study (Zhang and Li 2015), $\rho_{2.5,dry}$ is fixed to 1.5 g cm^{-3}, and $VE_f(FMF)$ and $f_o(RH)$ have been preliminarily defined as

$$VE_f(FMF) = 0.2887(FMF)^2 - 0.4663(FMF) + 0.356 \quad (2)$$

$$f_o(\mathrm{RH})=[1-(\mathrm{RH}/100)]^{-1} \tag{3}$$

By introducing Equations (2) and (3) into Equation (1), we can see that the PMRS method only needs four input parameters (including AOD, FMF, PBLH and RH) to estimate ground-level $PM_{2.5}$. Thus the procedure to obtain these four parameters is also the procedure to estimate $PM_{2.5}$.

2.2. Data acquisition

2.2.1. AOD from the GOCI satellite instrument

GOCI is a geostationary satellite instrument, so it can provide multi-temporal images with constant viewing angles. Therefore, we retrieve AOD using the multi-temporal method based on a look-up table (LUT) approach that is generally used in aerosol retrievals from satellite such as the well-known aerosol algorithm of MODIS (Remer et al. 2005). Considering directional effects, we apply multi-temporal images with the same UTC time, but different dates. Within a short date interval, such as one day, solar angles vary slowly. The solar illumination and satellite viewing geometry of GOCI images is approximately constant, which can considerably reduce the influence of directional effects in the retrieval. The multi-temporal method retrieves AOD by means of a priori knowledge that aerosol optical property can vary quickly with time but slowly with location, and that surface reflectance (SR) can vary quickly with location but slowly with time (Hagolle et al. 2015). According to the prior knowledge, the AOD of each pixel in a small image patch (e.g., 2 pixels × 2 pixels) is likely to have the same value, and the differences in the top-of-atmosphere (TOA) reflectance among pixels can likely be attributed to the differences in SR. Similarly, the SR of each pixel in the same location between two adjacent images in a short time is likely to have the same value, and the differences in the TOA reflectance among pixels can likely be attributed to the differences of AOD.

The LUT is precalculated for GOCI sensor and generated by using the 6S radiation transfer mode. The LUT is a simulation of the atmospheric contribution to the TOA reflectance. The TOA reflectance at the wavelength λ can be is described by:

$$\rho_{\mathrm{TOA}}(\mu_s,\mu_v,\varphi)=\rho_0(\mu_s,\mu_v,\varphi,\tau_a)+\frac{T(\mu_s,\tau_a)T(\mu_v,\tau_a)\rho_s(\mu_s,\mu_v,\varphi)}{1-S(\tau_a)\rho_s(\mu_s,\mu_v,\varphi)} \tag{4}$$

where ρ_{TOA} is TOA reflectance; $\mu_s=\cos\theta_s$, $\mu_v=\cos\theta_v$, θ_s and θ_v are solar zenith angle and satellite zenith angle, respectively; φ is solar and satellite relative azimuth angle, τ_a is AOD of a small image patch, in which each pixel has the same AOD; ρ_0 represents the atmospheric path reflectance, including aerosol and molecular contributions; $T(\mu_s,\tau_a)$ and $T(\mu_v,\tau_a)$ are transmittances for upward and downward radiation, respectively; $S(\tau_a)$ is the spherical albedo of atmosphere; ρ_s is SR. Equation (4) can be transformed and expressed as:

$$\rho_s=\frac{[\rho_{\mathrm{TOA}}(\mu_s,\mu_v,\varphi)-\rho_0(\mu_s,\mu_v,\varphi,\tau_a)]/T(\mu_s,\tau_a)T(\mu_v,\tau_a)}{1+S(\tau_a)[\rho_{\mathrm{TOA}}(\mu_s,\mu_v,\varphi)-\rho_0(\mu_s,\mu_v,\varphi,\tau_a)]/T(\mu_s,\tau_a)T(\mu_v,\tau_a)} \tag{5}$$

When the atmospherical model and the solar and satellite viewing geometry are given, in Equation (5), ρ_0, $T(\mu_s)T(\mu_v)$ and S are one-to-one correspondence with AOD and can be simulated together with AOD.

Equation (5) means that there is a nonlinear relationship between SR and AOD when TOA reflectance from the satellite observation is known. Two variables in an equation are unknown, which is mathematically an ill-posed inversion problem. Hence, it is necessary to make use of the prior knowledge to form a constraint. For each pixel of a small image patch (e.g., 2 pixels × 2 pixels) in one image, an equation can be established by using Equation (5), and for each pixel in another image, such equations can also be established. Since the SR in the same location between two images has the same value, we can establish at least four uncorrelated equations that contain only two AOD unknowns without SR. Thus, the number of equations is more than unknowns. We can compute the AOD values by solving

$$\tau^*, \tau'^* = \underset{\tau,\,\tau'}{arg\,min} \sum_{i\in\Omega} \left[\rho_s(\rho_{TOA}(i), \tau) - \rho_s(\rho'_{TOA}(i), \tau')\right]^2 \tag{6}$$

where i is the coordinate of pixels in a small image patch Ω, in which each pixel has the same AOD; $\rho_{\mathrm{TOA}}(i)$ and $\rho'_{\mathrm{TOA}}(i)$ are TOA reflectances from satellite observations on date D and date D′ at pixel coordinate i, respectively; τ and τ' are AODs of the patch Ω to be retrieved on D and D′, respectively; τ^* and τ'^* are retrieved AODs of the patch Ω on D and D′, when this quadratic objective is minimized by τ and τ'.

In this study, all the images are resampled into a 1.5 km spatial resolution. The patches of 2 pixels × 2 pixels are used in Equation (6), and AOD is considered to be a constant in the 3 km × 3 km areas. According to the TOA reflectances from satellite observations and solar-satellite geometry at each pixel of the patch, the different values of AOD and corresponding SR can be derived by using the LUT. The different values of SR are input into Equation (6). When the quadratic objective is minimized (i.e., the differences between SR of D and D′ are minimized), AOD and corresponding SR approach actual values. AODs of the patch on two images in time series can be retrieved at a 3 km resolution. Using LUT generated by 6S to retrieve AOD, we invariably acquire AOD at 550 nm regardless of what band data we choose.

In the actual retrieval, there may be some special cases, such as low AOD differences between two consecutive images. The initial SR term derived from SR products of other satellites (e.g., MODIS) may be considered to be added to Equation (6) to improve the robustness of multi-temporal method if it is possible.

2.2.2. FMF retrieval

FMF derived from satellite remote sensing represented by MODIS is the contribution of the fine model to the total AOD after the combination of the fine mode and coarse mode that are all bimodal models (Levy, Remer, and Dubovik 2007). This study adopts the definition of FMF in MODIS algorithm. We apply the LUT approach to achieve the combination of a fine model and a coarse model. We adopt the aerosol model from well-known global aerosol models of MODIS algorithm. Moderately absorbing aerosol model is selected as a fine model in winter and spring over Beijing area, while weakly absorbing aerosol model in summer and autumn, and dust aerosol model is selected as a coarse model in each season. The detailed model parameter values can be available from the work of Levy et al. (2013). Fine model parameters are defined in 6S and fine model LUT is generated by 6S. Similarly, coarse model LUT is also generated. A weighting parameter

(i.e., FMF) is defined between 0 and 1. The TOA reflectances of a fine model and a coarse model within LUT, which have the same wavelength, solar and satellite viewing geometry and aerosol optical depth, are weighted average according to the weighting parameter. The LUT approach to combine a fine model and a coarse model can be described by:

$$\rho_{TOA}^{LUT}(\tau_{550},\lambda)=\eta\rho_{TOA}^{f}(\tau_{550},\lambda)+(1-\eta)\rho_{TOA}^{c}(\tau_{550},\lambda) \quad (7)$$

where λ is the wavelength; η is FMF; ρ_{TOA}^{f} is TOA reflectance of a fine model; ρ_{TOA}^{c} is TOA reflectance of a coarse model; ρ_{TOA}^{LUT} is the combinational TOA reflectance that is the weighted average of the TOA reflectances of a fine model and a coarse model. τ_{550} is AOD at 550 nm and ρ_{TOA}^{f}, ρ_{TOA}^{c} and ρ_{TOA}^{LUT} have the same τ_{550} and λ.

Due to the lower accuracy of VE_f when FMF is lower than 0.1 in PMRS method, for FMF < 0.1, we assume FMF = 0.1 and therefore the range of FMF is set at 0.1–1.0, with 0.1 intervals and a total of 10 grades. The combinational TOA reflectance corresponds to the aerosol models weighted by FMF. If the AOD is retrieved from the combinational TOA reflectance calculated according to Equation (7) within LUT, the AOD and the corresponding FMF can be derived simultaneously. Instead of using the LUT from a constant aerosol model, the multi-temporal method uses the LUT from a combination of models with an unknown parameter FMF (i.e., the combinational LUT), which means that an unknown variable is added in AOD retrieval. Hence, it is necessary to add an additional GOCI band as a constraint to retrieve AOD and FMF simultaneously. After sensitivity analysis to FMF, GOCI band 3 (490 nm) and band 8 (865 nm) are finally selected for AOD and FMF retrieval because of their better performance to FMF than other bands.

We construct the combinational LUTs of band 3 and band 8, respectively, which differ only in the wavelength defined in 6S. Atmospheric profiles such as midlatitude summer and midlatitude winter are selected. The LUTs are calculated up to a τ_{550} of 5.0 (0.01, 0.25, 0.5, 0.75, 1.0, 1.5, 2.0, 3.0 and 5.0) and a ρ_s of 0.8 (0, 0.04, 0.08, 0.12, 0.16, 0.2, 0.24, 0.28, 0.32, 0.4, 0.6 and 0.8). Geometrical inputs are $\theta_s = 0^\circ\sim66^\circ$ ($\Delta = 6^\circ$), $\theta_v = 30^\circ\sim66^\circ$ ($\Delta = 6^\circ$) and $\varphi = 0^\circ\sim180^\circ$ ($\Delta = 12^\circ$), respectively, where Δ is an interval of angle. The lookup parameters such as θ_s, θ_v, φ, ρ_0, $T(\mu_s)T(\mu_v)$, S, τ_{550} and ρ_s are included within the combination LUTs.

Band 3 data are applied to retrieve AOD using multi-temporal method based on its combinational LUT. AOD and corresponding FMF of its combinational LUT can be derived, which as input parameters are applied in band 8. The corresponding values of SR are derived and input into Equation (6). When the quadratic objective is minimized, AOD and FMF approach actual values. In this way, we apply data of bands 3 and 8 to achieve the AOD and FMF retrieval.

2.2.3. PBLH and RH

PBLH can be inferred from ground-based or from spaceborne such as the Cloud-Aerosol Lidar and Infrared Pathfinder Satellite Observation (CALIPSO) and Cross-Track Infrared Sounder (CrIS) onboard Suomi National Polar-Orbiting Operational Environmental Satellite System Preparatory Project (SNPP). Since PBLH shows strong spatiotemporal variability, there are various limitations with some of these datasets. Ground-based measurements are sparse in spatial coverage. The swath width of spaceborne such as CALIPSO is very narrow and the spatial coverage PBLH images from SNPP-CrIS soundings

have a coarse spatial resolution of 0.25° × 0.25°. As for the RH, currently, there are also not suitable remotely sensed products near the ground, with sufficient spatiotemporal resolution matching retrieved AOD from GOCI, although it can be derived from meteorological stations or some satellite retrievals of atmospheric profiles, such as MODIS's MOD07 product. In recent years, the Weather Research and Forecasting (WRF) model has been widely used due to its good performance in the simulation of meteorological fields. WRF based on the reanalysis datasets can simulate the PBLH and RH data that have the same spatiotemporal resolution as GOCI. WRF simulated data may be used as ideal substitution for the missed remote sensing measurements (Zhang and Li 2015).

WRF can produce the needed PBLH and RH data of running in the same spatiotemporal resolution with GOCI data, but it does not mean that multi-temporal spatial coverage of $PM_{2.5}$ concentrations can be estimated in one day. When aerosols are uniformly mixed and mostly confined within the planetary boundary layer, the PBLH (i.e., the daytime mixing layer height) can be used as a good surrogate to estimate the aerosol layer height. Owing to solar heating at sunrise, the boundary layer generally starts growing and reaches to a maximum height during the afternoon hours and uniform mixing of aerosols occurs with condition of the active convection within boundary layer. This usually occurs after 6:00 UTC under cloud-free conditions according to the diurnal cycle observation of PBLH (Huang et al. 2016). In this state, the PMRS method can work well. In addition, the image of 7:16 UTC from GOCI has a relatively large solar zenith angle in winter, which may cause abnormal retrieval of AOD because of the less solar radiation received by the earth's surface. Hence, the image of only 6:16 UTC is the best choice to estimate $PM_{2.5}$ concentrations. The WRF model is running at a 3 km resolution, and the output temporal step of WRF is set at 30 min. The output PBLH and RH data are interpolated to correspond to the GOCI imaging time.

3. Results and validation

3.1. PMRS method results

We choose the time period from 1 December 2016 to 3 January 2017 as the investigation period focusing on the 'moderate', 'moderately polluted', 'heavily polluted' and 'severely polluted' processes in the study area. Cloud-free GOCI images covering Beijing area are obtained from the Korea Ocean Satellite Centre (http://kosc.kiost.ac.kr/). The technical software for GOCI (GDPS) is used to complete image clipping and produce GOCI Level 2 products from which the longitude, latitude, solar zenith angle, satellite zenith angle and solar and satellite relative azimuth angle for each pixel can be derived. AOD and FMF are retrieved using multi-temporal method based on the combinational LUTs. PBLH and RH are simulated using WRF model.

Ground-level dry $PM_{2.5}$ concentrations at a 3 km resolution in various polluted processes are derived as shown in Figure 1. The distribution of GOCI-estimated $PM_{2.5}$ concentrations in Figure 1(b,d,f,h) is essentially consistent with that of haze on GOCI RGB images in Figure 1(a,c,e,g). There is a distinct trend of $PM_{2.5}$ concentrations, which is higher in the southeaster plain and lower in the northwester mountain area. Figure 1(b) shows that in the moderate process at 6:15 UTC on 15 December 2016, there might be a transport of clean air from the North. Within the traces of clean air transport, $PM_{2.5}$ value

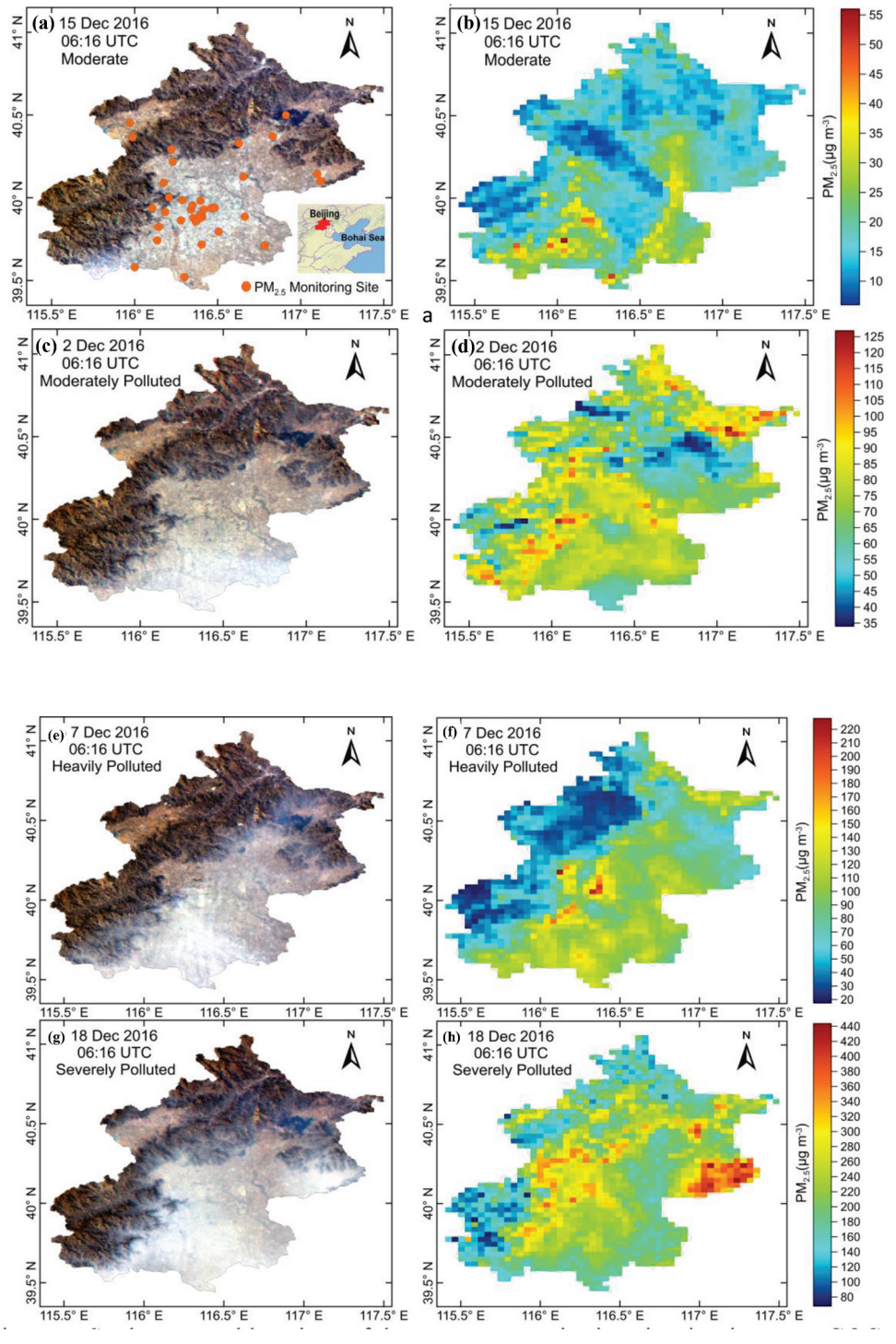

Figure 1. Study area and locations of the 35 $PM_{2.5}$ monitoring sites (a). GOCI-estimated $PM_{2.5}$ images showing various polluted processes (b, d, f and h). GOCI RGB images combined from three bands of 443, 555 and 660 nm in Figures 1a, 1 c, 1e and 1 g.

is below 20 μg m^{-3}, while outside it is as high as 55 μg m^{-3}. Figure 1(d,f,h) shows the processes of 'moderately polluted', 'heavily polluted' and 'serious polluted', respectively. It can be seen from the images that the terrain leads to unfavourable atmospheric diffusion. Haze accumulates heavily at the foot of the northwester mountains, and maximum $PM_{2.5}$ value in the area exceeds 440 μg m^{-3}.

3.2. Validation of $PM_{2.5}$ results

Hourly $PM_{2.5}$ validation data of 35 $PM_{2.5}$ monitoring sites (Figure 1(a)) are provided by Beijing Municipal Environmental Monitoring Centre (http://zx.bjmemc.com.cn). Two hundred and ninety-four valid in situ measurements ($N = 294$) in 9 sample days are obtained during the study period. We present the frequency distribution of $PM_{2.5}$ concentrations from GOCI and in situ measurements (Figure 2(a)). Figure 2(a) shows that GOCI-estimated results in general have good agreements with in situ measurements. The frequency differences between GOCI-estimated results and in situ measurements are less than 5%. The maximum frequency of in situ measurements lies on 0–50 μg m^{-3} with about 38% of the samples locating in this bin, while a close number (34%) of GOCI-estimated samples lie on the same bin. The frequency of GOCI-estimated results and in situ measurements appears at the third and fourth bin with an obviously lower frequency number than the others. This can be explained partly by the fewer pollution processes in the $PM_{2.5}$ range of 100–200 μg m^{-3} during the study period.

We also show a point-by-point validation of GOCI-estimated $PM_{2.5}$ and in situ measurements in Figure 2(b). The average GOCI-estimated $PM_{2.5}$ is 131.2 μg m^{-3} approaching 123.0 μg m^{-3} from in situ measurements. Mean of GOCI-estimated and in situ results is very close. The mean absolute error of all points is 41.8 μg m^{-3}, which is within our expectation comparing with a quite large $PM_{2.5}$ sampling range of 3–570 μg m^{-3}. Moreover, we found that GOCI-estimated results are underestimated when $PM_{2.5}$ values are higher and vice versa. The trend agrees with that frequency distribution in Figure 2(a). This can be explained by different spatiotemporal representativeness of both results. The GOCI-estimated results present the regional mean $PM_{2.5}$ over a square of about 3 km × 3 km, which is almost instantaneously observed. Yet, in situ measurements present hourly

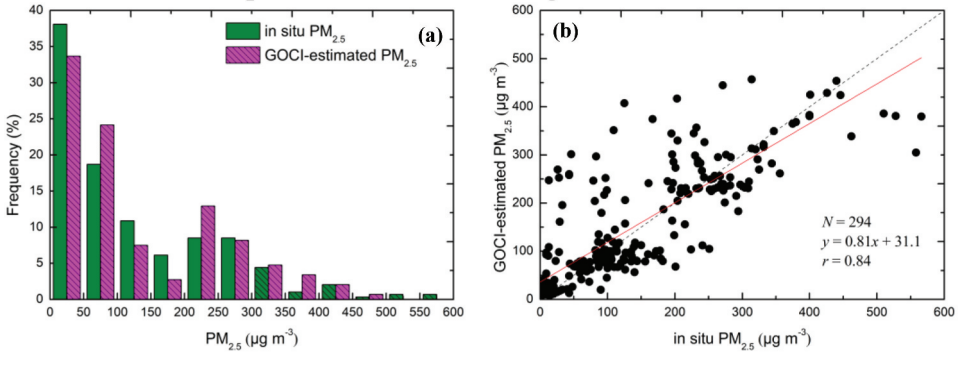

Figure 2. (a) Frequency distribution of $PM_{2.5}$ concentrations from GOCI and in situ measurements. (b) Comparison between GOCI-estimated $PM_{2.5}$ with in situ measurements.

averaged $PM_{2.5}$ values at $PM_{2.5}$ monitoring sites. A fairly good linear fit slope (0.81), relatively higher correlation coefficient (r = 0.84) and intercept of 31.1 μg m^{-3} confirm that GOCI has desirable performance in estimating $PM_{2.5}$ concentrations.

4. Conclusion

We introduce the approach using GOCI data to estimate ground-level dry $PM_{2.5}$ concentrations at a 3 km resolution over Beijing. We take advantage of the characteristic of GOCI's high temporal resolution. As only GOCI images acquired after the time when uniform mixing of aerosols occurs within boundary layer are used for $PM_{2.5}$ estimation, input data are more in line with the assumptions of PMRS method. Although the retrieved data (AOD, FMF) and simulated data (PBLH, RH) still have some uncertainties, the GOCI-estimated results show good agreements with in situ measurements. This suggests that the PMRS method can be employed to estimate $PM_{2.5}$ concentrations in various pollution processes based on GOCI, which is not dependent on rich historical data and geographical location. With the increase of multi-angular and polarization measurements, better satellite retrievals of aerosol parameters including PBLH and RH are expected to be released in the near future. GOCI will further demonstrate its latent capacity in air-quality monitoring.

Disclosure statement

No potential conflict of interest was reported by the authors.

Funding

This work was supported by the National Natural Science Foundation of China under Grant [Number 41671367].

References

Hagolle, O., M. Huc, D. Villa Pascual, and G. Dedieu. 2015. "A Multi-Temporal and Multi-Spectral Method to Estimate Aerosol Optical Thickness over Land, for the Atmospheric Correction of FormoSat-2, LandSat, VENμS and Sentinel-2 Images." *Remote Sensing*. 7(3):2668–2691.

Huang, M., Z. Gao, S. Miao, F. Chen, M. A. LeMone, J. Li, F. Hu, and L. Wang. 2016. "Estimate of Boundary-Layer Depth over Beijing, China, Using Doppler Lidar Data during SURF-2015." *Boundary-Layer Meteorology*. 162(3):503–522.

Levy, R. C., S. Mattoo, L. A. Munchak, L. A. Remer, A. M. Sayer, F. Patadia, and N. C. Hsu. 2013. "The Collection 6 MODIS Aerosol Products over Land and Ocean." *Atmospheric Measurement Techniques*. 6(11):2989–3034.

Levy, R. C., L. A. Remer, and O. Dubovik. 2007. "Global Aerosol Optical Properties and Application to Moderate Resolution Imaging Spectroradiometer Aerosol Retrieval over Land." *Journal of Geophysical Research*. 112:D13210. doi:10.1029/2006JD007815.

Li, Z., Y. Zhang, J. Shao, B. Li, J. Hong, D. Liu, D. Li, et al. 2016. "Remote Sensing of Atmospheric Particulate Mass of Dry $PM_{2.5}$ Near the Ground: Method Validation Using Ground-based Measurements." *Remote Sensing of Environment*. 173:59–68.

Lv, B., Y. Hu, H. H. Chang, A. G. Russell, J. Cai, B. Xu, and Y. Bai. 2017. "Daily Estimation of Ground-level $PM_{2.5}$ Concentrations at 4km Resolution over Beijing-Tianjin-Hebei by Fusing MODIS AOD and

Ground Observations." *Science of the Total Environment*. 580:235–244. doi:10.1016/j.scitotenv.2016.12.049.

Munchak, L. A., R. C. Levy, S. Mattoo, L. A. Remer, B. N. Holben, J. S. Schafer, C. A. Hostetler, et al. 2013. "MODIS 3 Km Aerosol Product: Applications over Land in an Urban/Suburban Region." *Atmospheric Measurement Techniques*. 6(7):1747–1759. doi:10.5194/amt-6-1747-2013.

Pang, J., Z. Liu, X. Wang, J. Bresch, J. Ban, D. Chen, and J. Kim. 2018. "Assimilating AOD Retrievals from GOCI and VIIRS to Forecast Surface $PM_{2.5}$ Episodes over Eastern China." *Atmospheric Environment*. 179(4):288–304.

Park, S., M. Shin, J. Im, C.-K. Song, M. Choi, J. Kim, S. Lee, et al. 2019. "Estimation of Ground-level Particulate Matter Concentrations through the Synergistic Use of Satellite Observations and Process-based Models over South Korea." *Atmospheric Chemistry and Physics*. 19(2):1097–1113. doi:10.5194/acp-19-1097-2019.

Remer, L. A., Y. J. Kaufman, D. Tanré, S. Mattoo, D. A. Chu, J. V. Martins, -R.-R. Li, et al. 2005. "The MODIS Aerosol Algorithm, Products, and Validation." *Journal of the Atmospheric Sciences*. 62 (4):947–973. doi:10.1175/jas3385.1.

Zhang, Y., and Z. Li. 2015. "Remote Sensing of Atmospheric Fine Particulate Matter ($PM_{2.5}$) Mass Concentration near the Ground from Satellite Observation." *Remote Sensing of Environment*. 160:252–262. doi:10.1016/j.rse.2015.02.005.

Zhang, Y., Z. Li, Y. Zhang, W. Hou, H. Xu, C. Chen, and Y. Ma. 2014. "High Temporal Resolution Aerosol Retrieval Using Geostationary Ocean Color Imager: Application and Initial Validation." *Journal of Applied Remote Sensing*. 8(1):083612.